Solar PV Power Output Prediction Using Sky Images

Hammad Hasan
Department of Electrical and Computer Engineering
Khalifa University
Abu Dhabi, United Arab Emirates
100062594@ku.ac.ae

Tarek H. M. El-Fouly
Department of Electrical and Computer Engineering
Khalifa University
Abu Dhabi, United Arab Emirates
tarek.elfouly@ku.ac.ae

***Abstract*—Solar photovoltaic (PV) installation is growing rapidly across the world, but the variability of solar power hinders its further penetration into the power grid. Part of the short-term variability stems from sudden changes in meteorological conditions, i.e., change in cloud coverage, which can vary PV output significantly in time scales of minutes. Images of the sky provide information on current and future cloud coverage, and are potentially useful in inferring PV generation. Sky-image-based solar forecasting using deep learning has been recognized as a promising approach for predicting short-term fluctuations.**

***Index Terms*—component, formatting, style, styling, insert**

I. Introduction

In 2021, solar photovoltaic (PV) generation experienced significant growth, reaching over 1000TWh with a record increase of 179TWh (22%) [1]. Solar PV is increasingly becoming the most cost-effective choice for new electricity generation in many regions worldwide, leading to anticipated investments in the years to come.

The rapid expansion of solar power faces obstacles when it comes to widespread implementation and replacing fossil fuels. Although the average output of solar photovoltaic (PV) systems over longer periods can be anticipated by considering daily and seasonal solar variations, short-term predictions are challenging due to unpredictable weather conditions, particularly cloud coverage. In situations where there are intermittent clouds, the output of PV systems can plummet to nearly zero within minutes [2]. Presently, short-term forecasts for PV output suffer from inadequate precision, and minute-level predictions in partly cloudy conditions often exhibiting substantial errors.

Accurate short-term PV forecasts have various applications. Generation utilities can use them for real-time market bidding strategies, transmission operators and balancing authorities can determine the need for operating reserves or ancillary services, and PV users can modulate power demand to avoid peak penalties based on cloud cover.

Sky images captured near a PV system can provide valuable information for predicting PV output. The position of the sun in the image correlates with theoretical insolation, while cloud distribution, color, and transparency impact light absorption and reflection. The movement and shape of clouds can even indicate future sky conditions and PV output. Extracting and understanding this information using explicit models is challenging. To address this, the study explores the use of deep learning techniques to learn the correlation between sky images and contemporaneous PV output. The focus is on assessing the correlation between images and current PV output, but the approach could be extended to using image sequences to predict future output.

II. Literature Review

Previous research on predicting PV output can be categorized into two main groups: models designed for clear sky predictions and models intended for general weather conditions, including sunny and cloudy scenarios.

In clear sky conditions, the changes in insolation and consequently the PV panel's output are primarily influenced by variations in the solar zenith angle and air mass. These fluctuations can be precisely characterized by employing clear sky models which are relatively simple equations like:

$$GHI = 1098 \cos(z) e^{\frac{-0.057}{\cos(z)}} \tag{1}$$

where GHI is global horizontal insolation (W/m^2), and z is the solar zenith angle in radians. The clear sky models that only utilize one parameter (like z) can get a relative Root Mean Square Error of $\approx$ 10% [3]. It is a very simple model with adequate accuracy for a clear sky.

Predicting PV output becomes more challenging under general weather conditions due to the unpredictable nature of weather or the atmosphere. This volatility primarily is due to the variations in cloud coverage, as well as to a lesser extent, fluctuations in water vapor content and aerosol concentration. These factors contribute to local and short-term effects that introduce significant uncertainty in forecasting the output of solar panels over short time intervals.

Previously, a simplified method has been proposed to model short-term fluctuations of sea surface insolation caused by cloud cover variations using cloud images collected on four research cruises [4]. The study in [5] presents a statistical analysis covering a span of four years (January 2006 - December 2009) to quantify the short-term variability of the total solar irradiance. The analysis focuses on different levels of cloudiness, which were determined by measuring the amount of cloud cover.

Artificial Neural Networks (ANN) have also been used previously to predict insolation. These ANN models are mostly based on Power Generation history rather than images. The author in [6] presents a term prediction method of generated power for small PV Power Stations based on self–organizing maps and previously introduced power profiles.

A paper in [7] introduces a least-square support vector machine (SVM) model for short-term solar power prediction (SPP). The model utilizes historical atmospheric data and other meteorological variables, such as sky cover, relative humidity, and wind speed, to predict solar power based on location and time. The author of [8] used ANN which directly takes the mean and variance of color intensity of cloud images as input. Only utilizing the statistical variables leaves out a lot of features that could be used using Convolutional Neural Networks (CNN).

III. Data and Models

Images captured by ground-based fish-eye cameras contain a wealth of information about the sky, but this information is challenging to extract and use for reliable predictions.

A. Sampling Images from Video Recordings

Video recordings of the sky during the day time are taken using a 6 megapixel (3072 × 2048) fish-eye camera with a field of view (FOV) of 360°. The camera is installed on the roof of the Green Earth Sciences Building (GESB) at Stanford University. The wide FOV of a fish-eye camera provides maximal information in a single frame.

As PV data is available at 1 min resolution, frames are snapshotted from the video with the same frequency at corresponding PV output times. Videos were collected from December 2016 to December 2019, with small interruptions due to wiring failure and/or electrical failure of the camera from excessive precipitation. Images are down-sampled to a resolution of 64 × 64 in our baseline case to reduce model training time.

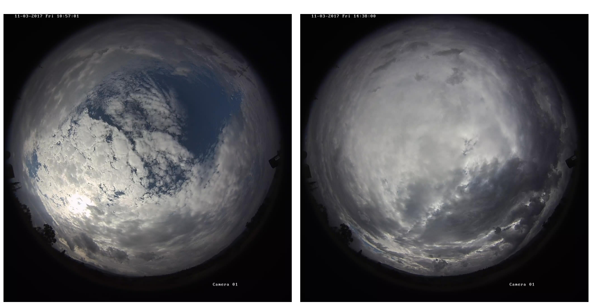

Fig. 1. Sample Image Outputs for the Fish Eye Camera

B. Solar Panel Outputs

The solar panel output data utilized in the study is obtained from a solar PV array located at a distance of 125m from the fish-eye camera. The recorded data from the panel output occasionally experiences sensor malfunctions, leading to missing or unreliable data for certain observation days. Therefore, it is necessary to apply a filtering process to eliminate inaccurate data and ensure the reliability of the PV output information.

Cloudy conditions cause a lot of variations in direct normal irradiation that diminishes electricity generation. An example can be seen in the following figure.

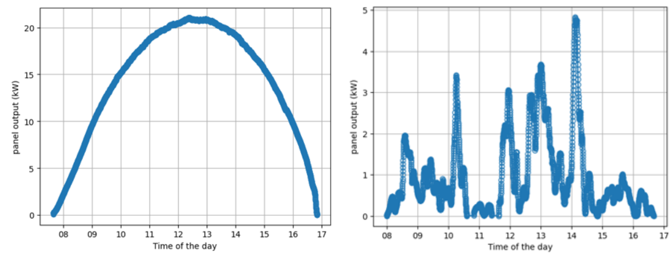

Fig. 2. Sample PV Output for a sunny day and cloudy day respectively.

These sample outputs are after filtering the night hours and missing values. The cloud image can be seen to have a lot of irregularities. The data is fairly balanced as can be seen in Figure 3.

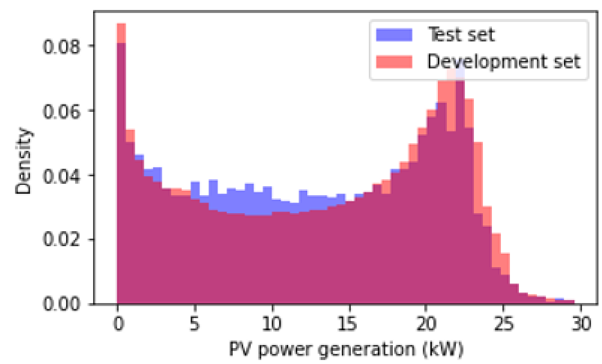

Fig. 3. Data Probability Density Distribution for Training and Testing

C. Data Preprocessing

A valid observation requires that the data should be available for both the PV output and the corresponding image at the same timestamp. The training data is divided into validation and testing data using 2-Fold Cross Validation, which divides the data equally and trains two models equally. These models are then ensembled to give the final predictions for the regression problem. The final number of matches can be seen in the following Table.

TABLE I
Dataset

PV Power	Images	Observations	Training	Testing
1482241	508807	363375	349372	14003

D. Models Using CNN Architecture

The models used with the data are VGG16 (end to end), VGG16 (ImageNet), ResNet, and Convolutional Neural Networks (CNN) with a fully dense layer connected at the end.

Further, these models also include max-pooling layers, batch normalization, and convolutional layers. At the end of the fully connected layers, a regression result is generated which predicts the PV output. The input image is passed sequentially into the network, after the convolution base the processed input is flattened into a vector and fed into several fully connected layers.

One of the CNN structures is shown in Figure. 8. The input images are initially processed through two ConvPool structures. Each Conv-Pool structure consists of a convolutional layer, a batch normalization layer, and a pooling layer, arranged in that sequence. The convolutional layer applies a 3×3 filter with a stride length of one and same-value padding. The activation function employed is Rectified Linear Unit (ReLU). Batch normalization is applied after convolution to enhance training speed and improve model robustness. A 2×2 max pooling operation is utilized in the pooling layer, which plays a crucial role in capturing translation-invariant features.

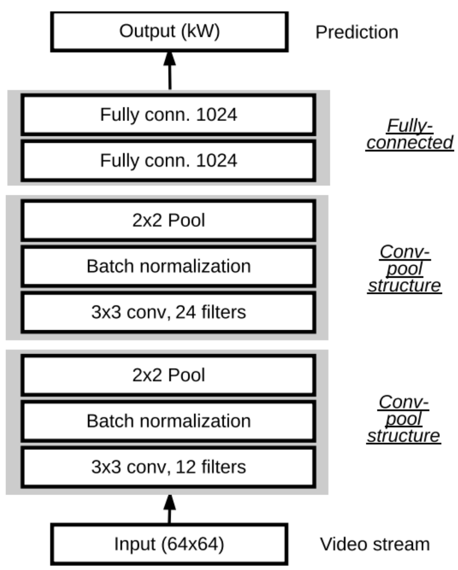

Fig. 4. Optimized CNN Structure

A stochastic gradient descent optimizer, Adam, is used to adjust the learning rate. Mean Squared Error of the PV Output prediction is used as the loss function to update the new weights after each iteration.

$$\text{Loss} = \frac{1}{N} \sum_{i \in S} (P_i - G_i)^2 \tag{2}$$

where S is the set of samples, N = —S— is the number of samples, P_i is the predicted output and G_i is the true output for sample i. The loss is measured in KW^2.

IV. Results

The Root Mean Squared Error (RMSE) and Mean Absolute Error (MAE) metrics are used to evaluate the performances of the different models.

$$RMSE = \sqrt{\sum_{i=1}^{n} \frac{(\hat{y}_i - y_i)^2}{n}} \tag{3}$$

$$MAE = \frac{1}{n} \sum_{i=1}^{n} |y_i - \hat{y}_i| \tag{4}$$

where $\hat{y}_i$ is the predicted value, y_i is the ground truth, and n is the number of samples.

A. Results for VGG16 with ImageNet

Training the last 2 convolution layers with 2 more dense layers to modify the old weights to the new data. The trainable parameters for this method are 4,459,009, and this model was trained for 5 epochs. The RMSE ranged from [0.6, 2.66] KW for a sunny day and RMSE ranged from [3.18, 6.66] KW for a cloudy day. One example of the result can be seen in the following figure with blue being the predicted output:

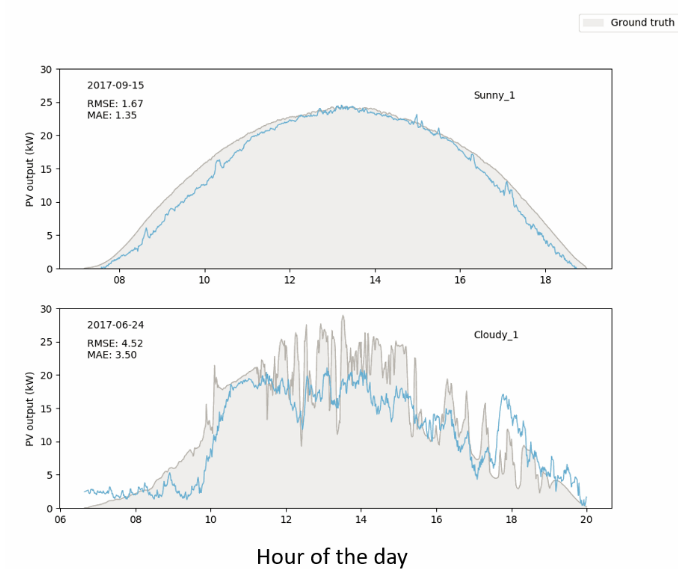

Fig. 5. Results for VGG16 (ImageNet)

B. Results for VGG16

Training the whole 16 convolutional layers of VGG16 along with 2 dense layers. The trainable parameters for this method are 15,239,489, and this model was trained for 4 epochs. The RMSE ranged from [0.21, 1.12] KW for a sunny day, which is a substantial improvement from the transfer learning approach. RMSE ranged from [1.68, 5.18] KW for a cloudy day. This can be seen as the most challenging part of this problem, as it is very difficult to predict the PV output with the intermittent nature of clouds. Results from this model are shown here:

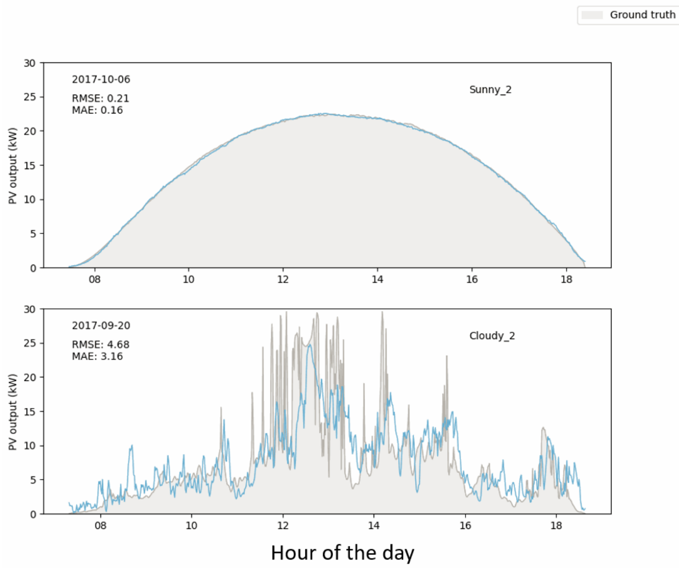

Fig. 6. Results for VGG16 (End to End)

C. Results for ResNet

This consists of one Residual Connection other than the common max-pooling, convolutional layer, and batch normalization. The trainable parameters for this method are 7,416,881, and this model was trained for 4 epochs. The RMSE ranged from [0.42, 2.58] KW for a sunny day, which is a substantial improvement from the transfer learning approach, but still not as good as end-to-end training for VGG16. RMSE ranged from [1.99, 4.92] KW for a cloudy day. Although it has lower trainable parameters than VGG16, the RMSE it got is lower than that of the VGG16. Results from this model are shown here:

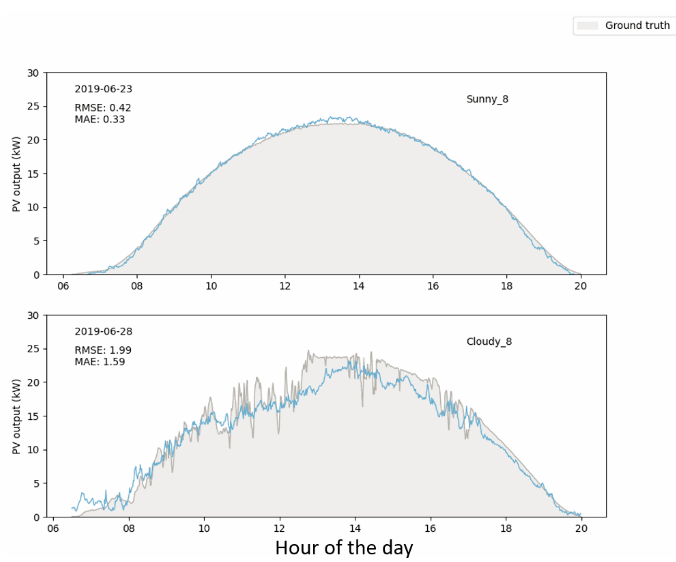

Fig. 7. Results for ResNet

D. Results for Optimized CNN

Training the whole 16 convolutional layers of VGG16 along with 2 dense layers. The trainable parameters for this method are 13,645,937, and this model was trained for 12 epochs. The RMSE ranged from [0.33, 1.16] KW for a sunny day. This model is not as good as the VGG16 (End to End), but the error is still lower than the other models. RMSE ranged from [1.83, 4.93] KW for a cloudy day. This was on par with ResNet, but it had almost double the training parameters. An example output of this model is shown below.

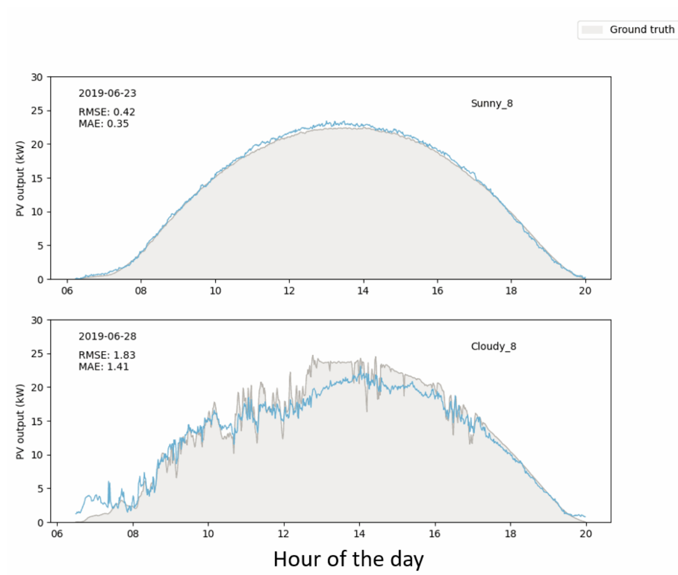

Fig. 8. Results for Optimized CNN

E. Comparisons

The table below shows the number of parameters in the models used above.

	Non-Trainable Params	Trainable Params	Total Params
VGG16(ImageNet)	12,354,880	4,459,009	16,813,889
VGG16	0	15,239,489	15,239,489
ResNet	336	7,416,881	7,417,217
Optimized CNN	144	13,645,937	13,645,937

Fig. 9. Model Paramters

All the errors are compiled in Figure 10, and it can be concluded that the VGG16 worked best for sunny days. For the cloudy days, there is no clear better model. Better model architecture must be trained to find a more effective model.

All the results in the table are in Kilowatts (KW).

	Sunny Days		Cloud Days		Overall	
	RMSE	MAE	RMSE	MAE	RMSE	MAE
VGG16(ImageNet)	1.253	0.934	4.599	3.541	3.374	2.241
VGG16	0.631	0.482	3.509	2.440	2.524	1.463
ResNet	1.324	1.017	3.640	2.665	2.741	1.843
Optimized CNN	0.742	0.599	3.392	2.383	2.458	1.493

Fig. 10. Overall Results

V. Future Work

A. Convolution Intermediate Activations

The input data was visualized after passing through the convolutional layers to figure out why the models were not working well in cloudy conditions. The third activations are shown here for the sunny and cloudy image. These results suggest that something like U-Net or other architecture should be used to capture the features of the cloudy sky.

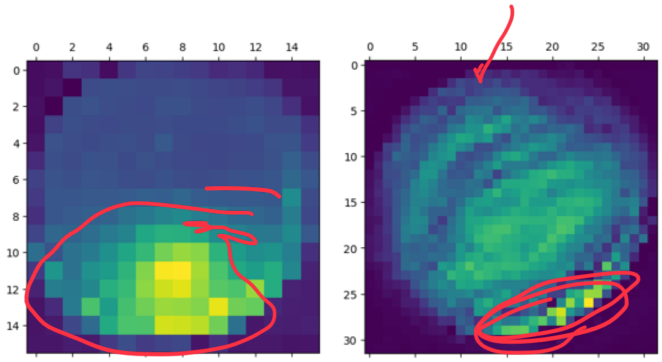

Fig. 11. Activation of Third Convolution Layer

B. Solar Forecasting

Time-series image data can be created to predict the future output of the PV Power Plant. The images can also be sampled at a higher frequency which could predict the output better for sudden changes. For forecasting, the time-series image requires a higher specification computer because of the large number of images. The PV data can be increased by interpolation or more data can be used from other facilities to build a large database and use the trained model to predict solar irradiance. Furthermore, other relevant factors such as temperature and humidity can be considered alongside solar irradiance to improve the predictive capability of the models.

VI. Conclusion

This paper predicts the solar panel output using sky images by using models based on convolutional neural networks and then the results are compared to find the best model. The developed models are working very well for sunny/clear sky conditions. For the cloudy specifications, the model does not perform well enough. The best-performing model for the clouds was the Optimized CNN model, but it was performing very close to VGG16 and ResNet.

The accuracy of the models could be further improved by creating time-series image data for a lower resolution than 1 minute. Increasing the number of layers (dense or convolutional) in the architecture gives us a little advantage. New models or structures can be developed for cloud-based regression. These models can be used to predict solar-irradiance in a more affordable way as compared to the traditional approaches.

References

[1] International Energy Agency (IEA), "Solar PV." https://www.iea.org/reports/solar-pv, 2022. License: CC BY 4.0.

[2] A. Zaher, S. Thil, J. Nou, A. Traoré, and S. Grieu, "Comparative study of algorithms for cloud motion estimation using sky-imaging data," *IFAC-PapersOnLine*, vol. 50, no. 1, pp. 5934–5939, 2017. 20th IFAC World Congress.

[3] J. S. Stein, C. W. Hansen, and M. J. Reno, "Global horizontal irradiance clear sky models : implementation and analysis.," 3 2012.

[4] J. Kalisch and A. Macke, "Estimation of the total cloud cover with high temporal resolution and parametrization of short-term fluctuations of sea surface insolation," *Meteorologische Zeitschrift*, vol. 17, pp. 603–611, 10 2008.

[5] M. Antón, J. Gil, A. Cazorla, J. Fernández-Gálvez, I. Foyo-Moreno, F. Olmo, and L. Alados-Arboledas, "Short-term variability of experimental ultraviolet and total solar irradiance in southeastern spain," *Atmospheric Environment*, vol. 45, no. 28, pp. 4815–4821, 2011.

[6] M. Radvanský, M. Kudělka, and V. Snášel, "Short term power prediction of the photovoltaic power station based on power profiles," in *Proceedings of the Fifth International Conference on Innovations in Bio-Inspired Computing and Applications IBICA 2014* (P. Kömer, A. Abraham, and V. Snášel, eds.), (Cham), pp. 383–393, Springer International Publishing, 2014.

[7] J. Zeng and W. Qiao, "Short-term solar power prediction using a support vector machine," *Renewable Energy*, vol. 52, pp. 118–127, 2013.

[8] Y. Chu, M. Li, H. T. Pedro, and C. F. Coimbra, "Real-time prediction intervals for intra-hour dni forecasts," *Renewable Energy*, vol. 83, pp. 234–244, 2015.

[9] Y. Nie, X. Li, A. Scott, Y. Sun, V. Venugopal, and A. Brandt, "SKIPP'D: a SKy Images and Photovoltaic Power Generation Dataset for Short-term Solar Forecasting," *arXiv preprint arXiv:2207.00913*, 2022.

[10] Y. Sun, G. Szűcs, and A. R. Brandt, "Solar pv output prediction from video streams using convolutional neural networks," *Energy Environ. Sci.*, vol. 11, pp. 1811–1818, 2018.

[11] H. Farouk, R. Hamid, H. K. Elminir, and A. Abulwfa, "Ground-based measurements of uv index (uvi) at helwan," *NRIAG Journal of Astronomy and Geophysics*, vol. 1, no. 2, pp. 159–164, 2012.

[12] S. University, "2017-2019 sky images and photovoltaic power generation dataset for short-term solar forecasting (stanford benchmark)." https://purl.stanford.edu/td987qz8378, 2020. Accessed: 2023-05-13.